Thermal Science and Engineering (2020) Volume 3 Issue 1
doi:10.24294/tse.v3i1.515

ORIGINAL RESEARCH ARTICLE

Cross-wire projection welding of Aluminium alloys in relation to pneumatic and electromechanical electrode force systems

Zygmunt Mikno

Welding Institute, Gliwice, Poland. Email: zygmunt.mikno@is.gliwice.pl

ABSTRACT

The cross-wire projection welding of wires (Al 5182, = 4 mm) performed using the conventional (i.e. pneumatic) electrode force system was subjected to thorough numerical analysis. Calculations were performed until one of adopted boundary conditions, i.e., maximum welding time, maximum penetration of wires, the occurrence of expulsion or the exceeding of the temperature limit in the contact between the electrode and the welded material was obtained. It was observed that the ring weld was formed within the entire range of welding parameters. The process of welding was subjected to optimization through the application of a new electromechanical electrode force system and the use of a special hybrid algorithm of electrode force and/or displacement control. Comparative numerical calculations were performed (using SORPAS software) for both electrode force systems. Technological welding tests were performed using inverter welding machines (1 kHz) provided with various electrode force systems. The research also involved the performance of metallographic and strength (peeling) tests as well as measurements of welding process characteristic parameters (welding current and voltage).

The welding process optimization involving the use of the electromechanical force system and the application of the hybrid algorithm of force control resulted in (1) more favorable space distribution of welding power, (2) energy concentration in the central zone of the weld, (3) favorable (desired) melting of the material within the entire weld transcrystallisation zone and (4) obtainment of a full weld nugget.

Keywords: FEM; Resistance Welding; Projection Welding; Electromechanical Force System

ARTICLE INFO

Received: 5 February 2020
Accepted: 14 March 2020
Available online: 21 March 2020

1. Introduction

Force is one of the three primary technological parameters of a welding process. The other two parameters are the value of current and the time of current flow. During cross wire projection welding (particularly of aluminum alloys) in a conventional application i.e. using a pneumatic force system, it is very difficult to make a weld with a full weld nugget. The pneumatic force system is characterized by high inertia and cannot be applied changes in force are or must be fast. For this reason, the value of pre-set force is usually constant. If the force is excessively high, the high deformation of welded elements (wires) may occur as a result. If the force is overly low, the formation imperfections of a projection joint (high temperature in contacts, expulsion) may follow[1]. In the pneumatic system, force applied during welding results from specific force pre-set by a pneumatic cylinder. The displacement of electrodes results from the action of this force and of the changeable mechanical resistance of materials being welded.

An alternative solution requires another method enabling the exerting of force on materials subjected to welding[1-6]. In publication[1], the authors emphasize the growing popularity of the servomechanical

(electromechanical) system and an advantage involving an increase in an electrode displacement rate during welding. Publication[2] informs about the possible extension of the window of technological parameters, improving the weldability of materials. Work[3] refers to the possible modulation of force and its fast changes, particularly at the end of the process of welding. Gould[4] emphasized an increase in electrode service life in spot resistance welding and the use of servomotors in the riveting technology. Work[5,6] stated that the electromechanical (servomechanical) system eliminated the dynamic impact of electrodes against a material subjected to welding (during initial force), which was characteristic of pneumatic actuators. The electromechanical systems enabled a gentle "touch" of an electrode against a material being welded. Publication[6] enumerates other advantages of the electromechanical system including (1) superior (faster) operation of a welding gun (servo) in space, (2) greater repeatability of force, (3) reduced noise, (4) shorter welding time and (5) shorter movement during the closing and opening of the electrodes, extending the service life of mechanisms.

In the solution analysed in this paper, i.e. involving the use of the electromechanical force system, the displacement of electrodes is pre-set and resultant force depends on the displacement of electrodes and the resistance of the deformation of a contact area being heated. Available reference publications do not contain information concerning such a method of electrode movement control as the method presented in this study.

The authors of publications[7,8] describe a new control system and the results of its operation, particularly visible in projection welding. Publication[7,9] presents a new control system used during the welding of sheets with an embossed projection. Another application of the new solution, i.e. cross wire welding is presented in publication[10].

Publications[7-10] present an entirely different solution, i.e. the slowing down of the displacement of an electrode during the projection welding of sheets with an embossed projection. This approach is new and characterized by advantages which are worth a mention. The above-named idea can be used in another projection welding technology, i.e. cross wire welding. It is possible to reduce the penetration of wires and to generate more energy in the most desirable place, i.e. in the contact area between wires. The new idea of electrode displacement control significantly changes the previous approach to the course of the resistance welding process (projection cross wire welding) and significantly affects the development of the entire research area (pressure welding).

The article constitutes a fragment of greater research, where the process of welding is analysed in respect of the application of variable electrode force or electrode displacement control. The new method of control is performed using the electromechanical force system. Research-related tests described in the article involved the use of the SORPAS 3D computational model.

Table 1. Simulation parameters

Time step increment	**Squeeze**	**Up-slope**	**Weld**	**Hold**	
Pneumatic force system	10	3	40	100	ms
Electromechanical force system	10	3	60	100	ms
Time step	0.1	0.1	0.1	1	ms
Convergence control					
Convergence accuracy					
Electrical model	1.00E-5				
Thermal model	1.00E-5				
Mechanical model	1,00E-5				
Dynamic contact between objects	Sliding				
Heat loss to the environment					
Air temperature	20				°C
Heat transfer rate	300				W/m^2*K
Electrode dimensions					
Length x width	10.0 × 8.0				mm
Electrode height	5				mm
Welding current	DC				

2. FEM calculations

The research-related FEM calculations were conducted using the SORPAS 3D software mode[11]. The software programme enables the performance of related analyses, including coupled electro-thermo-mechanical-metallurgical analyses. The above-named software features a module including the effect of a new force and a precise electrode movement solution, i.e. based on the electromechanical system.

Simulation parameters used in the study and involving the use of the FEM computational software are presented in **Table 1.**

A cross-wire projection welded joint made using the pneumatic electrode force system is characterised by a thin layer a molten material (metal subjected to welding). Usually, a weld is formed in the solid state at a temperature below the melting point. The foregoing results from the specific nature of the process, i.e., the melting of the material and the pushing of the plasticised material outside the weld (joint) by constant and unfavourably excessive force. The weld adopts the shape as presented in **Figure** 错误!未找到引用源。**a)**; such a weld is referred to as a ring weld. As can be seen, the material in the central part of the weld is not molten (**Figure** 错误!未找到引用源。**b)**).

The research-related calculations and experimental tests involved the use of aluminium wires grade Al 5182 having a solidus temperature of 577 °C and a liquidus temperature of 638 °C.

3. Calculation model

The 3D model used when performing numerical calculations of the resistance projection cross wire welding is presented in **Figure 2**. The model-related assumptions involved copper electrodes (A2/2), welded material – aluminium wires grade AA5182[11] having a diameter of 4 mm and a length of 6 mm (**Figure 2a)**). The 3D model was composed of 11,083 mesh nodes and 9,404 elements. To provide necessary computational accuracy, the mesh was concentrated in the bar contact area (**Figure 2b)/c)**).

The analysis involved both the pneumatic and the electromechanical electrode force system. Criteria adopted when performing calculations were the following:

(1) obtainment of a nominal weld nugget diameter of 1.6 mm,

(2) bar penetration depth-max. 20% of the thickness of elements subjected to welding (Δl = 1.6 mm),

(3) lack of expulsion,

(4) lack of visible bar deformation (bending),

(5) maximum main current flow time of 63 ms (3 ms up-slope, 60 ms main time),

(6) maximum temperature in the contract area between the electrode and the welded material of 500 °C.

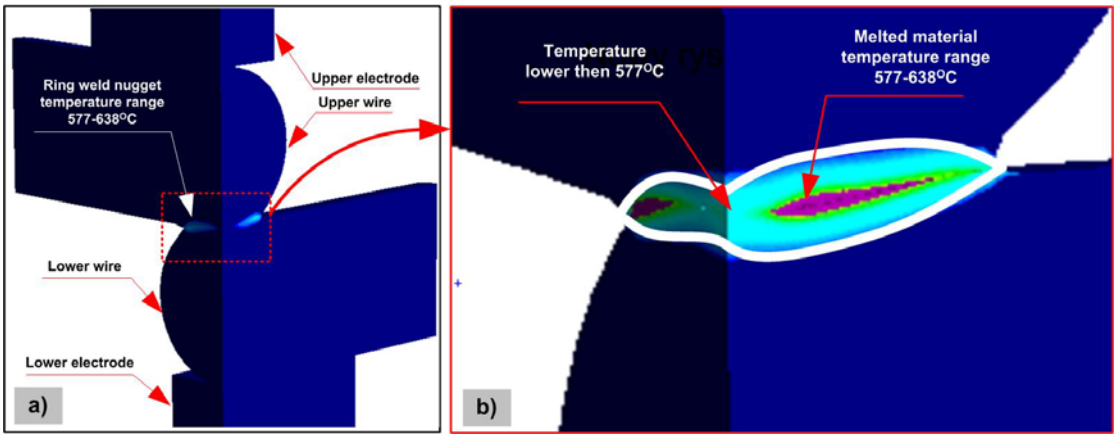

Figure 1. Temperature distribution in the welding area (3D model).

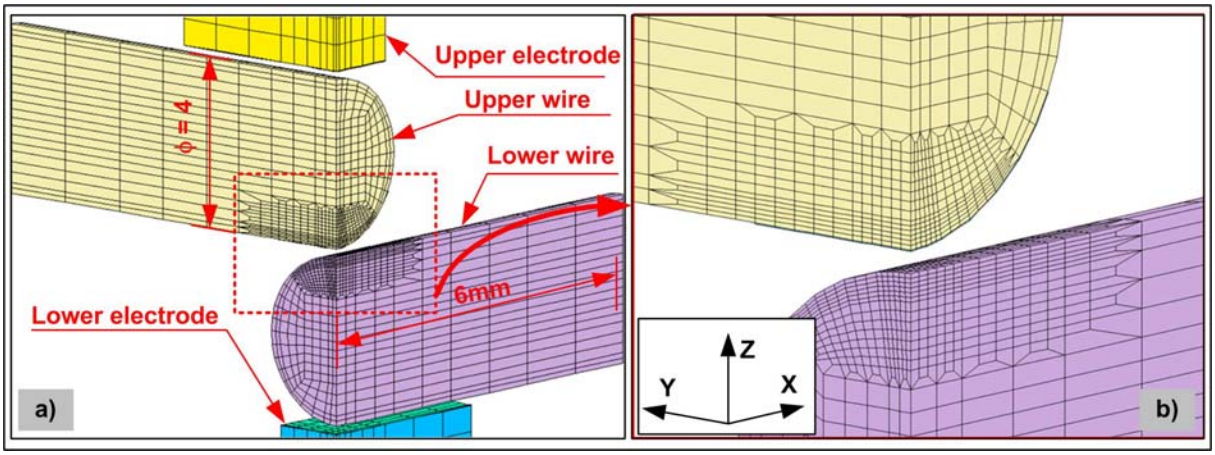

Figure 2. Geometry of the 3D model of cross wire welding (Al 5182).

The FEM calculations involved the adoption of material data form the software programme database (SORPAS)[11]:

(1) Aluminium wires Al 5182—designation of SORPAS AA5182(O) material database: Al 95 Mn 0.25 Mg 4.5, solidus: 577 °C, liquidus: 638 °C (**Table 2**).

(2) Electrodes grade A2/2 CuCrZr (**Table 3**).

Table 2. Material parameters of wires Al 95 Mn0.25, Mg4.5, solidus 577 °C, liquidus 638 °C[12]

Temperature	Thermal conductivity	Temperature	Heat capacity	Temperature	Resistivity	Temperature	Mass density	Temperature	Thermal expansion coefficient	Temperature	Young's modulus of elasticity
°C	W/m*K	°C	J/kg*K	°C	mΩ*m	°C	kg/m^3	°C	10^{-6}/°C	°C	kN/m^2
25	123.0	23	794	25	0.056	25	2660	25	23.9	25	70.0
100	134.0	50	825	100	0.068			250	25.0		
200	147.6			200	0.079						
400	160.9			400	0.103						
500	164.3			500	0.115						
600	163.3			600	0.131						

Table 3. Material parameters of electrodes ISO 5182 A2-2 Electrode CuCrZr

Temperature	Thermal conductivity	Temperature	Heat capacity	Temperature	Resistivity	Temperature	Mass density	Temperature	Thermal expansion coefficient	Temperature	Young's modulus of elasticity
°C	W/m*K	°C	J/kg*K	°C	mΩ*m	°C	kg/m^3	°C	10^{-6}/°C	°C	kN/m^2
20	326.6	20	372	20	0.022	20	8890	25	16.5	25	117.0
100	342.1	127	402	100	0.027	1080	8320				
300	338.0	327	422	200	0.038						
500	340.3	527	438	300	0.042						
700	332.0	727	456	400	0.049						
900	321.8	927	485	500	0.057						
				600	0.065						
				700	0.073						
				800	0.082						
				900	0.091						
				1000	0.102						
				1100	0.220						

4. Process parameters

On the basis of related standards and instructions, the following welding parameters were as-

sumed: (1) current intensity I = 8/9/10/11/12 kA, up-slope 3 ms + main welding time (maximum) 60 ms[12-14], (2) force F = 1.5/1.25/1.0/0.75/0.5 kN in relation to the pneumatic force system and (3) displacement control in relation to the electromechanical system. The remaining welding technology parameters included an initial squeeze time of 10 ms, a final squeeze time of 500 ms and the use of a DC inverter welding machine (1 kHz).

Table 4 presents pre-set parameters and characteristic parameters of selected variants used in the numerical calculations. The variants related to the pneumatic system are designated as P1–P9, whereas those related to the electromechanical systems are designated as E1–E3.

The analysis of the welding process involving the use of the pneumatic force system aimed to test and present the course of the variability of resultant process parameters and to identify the most favourable welding conditions. The results obtained in the analysis revealed the lack of welding process monotonicity in relation to a force of 0.75 kN. For this reason, it was necessary to perform additional calculations in relation to a force of 0.7 kN and that of 0.8 kN. In total, the welding process was analysed at 35 points (I = 8, 9, 10, 11, 12 kA and F = 1.5, 1.25, 1.0, 0.8, 0.75, 0.7 and 0.5 kN).

The numerical optimisation of the process was performed in relation to the electromechanical force system and lower values of welding current analysed in relation to the pneumatic system (8/9/10kA). The numerical calculations were performed until one of the (six) previously adopted boundary criteria was obtained.

The analysis of the PFS-related results in **Table 4** revealed that it was not possible to obtain a proper weld nugget within the analysed range of current (8.0–12.0 kA) and electrode force (1.5–0.5 kN).

Table 4. Pre-set parameters and characteristic parameters of selected variants in numerical calculations

No.	Variant	Current	Welding time	Force	Penetration Δl	Weld diameter	Weld volume	Energy	Remarks
		kA	ms	kN	mm		mm^3	kJ	
	1	2	3	4	5	6	7	8	9
Pneumatic system									
1	P1	8.0	63	1.5	1.47	0.1	0.0	0.17	overly small weld nugget diameter
2	P2	10.0	46		2.38	0.1	0.0	0.17	excessive penetration of bars
3	P3	12.0	29		1.85	0.0	0.0	0.15	
4	P4	8.0	63	1.0	1.00	0.2	0.0	0.20	overly small weld nugget diameter
5	P5	10.0	59		2.13	1.5	0.9	0.23	most favourable welding conditions
6	P6	12.0	46		2.54	0.2	0.0	0.30	in spite of significant penetration of bars
7	P7	8.0	63	0.5	0.57	0.3	0.1	0.25	overly small weld nugget diameter
8	P8	10.0	8		0.19	1.5	0.7	0.07	unfavourably short welding time, high dynamics of the force system required
9	P9	12.0	5		0.15	0.8	0.1	0.05	overly small weld nugget diameter
Electromechanical (servo) system									
10	E1	8.0	38	servo force	0.6	1.95	4.5	0.16	OK, full weld nugget, nugget diameter > 1.6 mm, penetration of bars < 1.6 mm
11	E2	9.0	25		1.2	2.00	5.3	0.10	
12	E3	10.0	2		1.5	2.20	5.6	0.13	

Note: red color—unacceptable param., green color—acceptable param., orange color—the most-beneficial welding conditions.

5. FEM calculation results

5.1 Calculation results related to the pneumatic system

The results of numerical calculations in relation to the pneumatic force system are presented in **Figure 3** and in **Table 5**. The numerical calculation results are presented in spatial charts developed using the Statistica software programme[15]. **Figure 3** (in the form of a surface chart) presents the formation of a weld nugget (**Figure 3a)**), welding time

(**Figure 3b)**), bar penetration depth (electrode displacement) (**Figure 3c)**) and energy supplied during welding (**Figure 3d)**). Dependences are presented in relation to various values of welding current and electrode force.

Numerical values related to the graphic presentation of the results shown in **Figure 3a)–3d)** are presented in **Table 5a)–5d)**. **Table 5e)–5g)** contains the following additional information concerning:

– obtained criterion (**Table 5e)**), i.e.:

– t—maximum heating time (current flow time, 63 ms),

– D—maximum electrode displacement (1.6 mm, 20% of the bar thickness),

– E—expulsion,

– weld (**Table 5f)**), i.e.:

– L—weld nugget diameter below 0.7 mm,

– R—ring-shaped weld nugget (0.7 mm < D (weld nugget diameter) <= 1.5 mm,

– F—full weld nugget (1.90 mm < D (weld nugget diameter)),

– weld nugget volume (**Table 2**).

The results presented in **Table 5** supplement the information concerning the course of the variability of characteristic parameters presented in **Figure 3**. The conclusions based on the analysis of the results presented in **Figure 3** and **Table 5** are the following:

– maximum obtainable weld nugget diameter amounted to 1.5 mm (**Table 5a)**—parameter field 1),

– within the entire range of the variability of welding current and electrode force parameters, including the largest obtained weld nugget diameters, i.e., from 1.0 mm to 1.5 mm, the obtained weld was ring-shaped (ring weld) (**Table 5f)**—parameter field 2),

– criterion of the exceeding of the maximum time of welding current flow (63 ms) was observed in relation to lower welding current values (**Table 5b)**—parameter field 3a, **Table 5e)**—parameter field 3b),

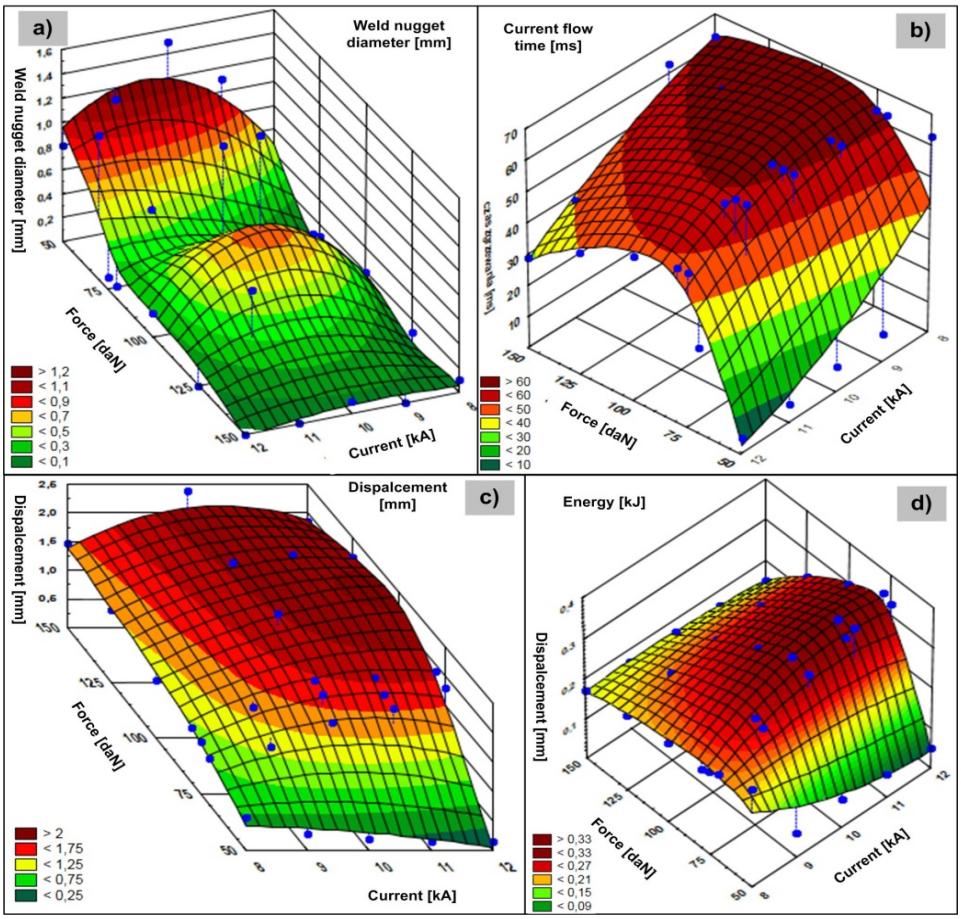

Figure 3. Course of the variability of characteristic parameters in relation to the pneumatic force system (Al 5182, ϕ = 4.0 mm). **a)** weld nugget diameter, **b)** current flow time, **c)** electrode displacement (penetration of wires), **d)** energy supplied to the weld**.**

Table 5. FEM calculation results in relation to cross wire welding (AL 5182)

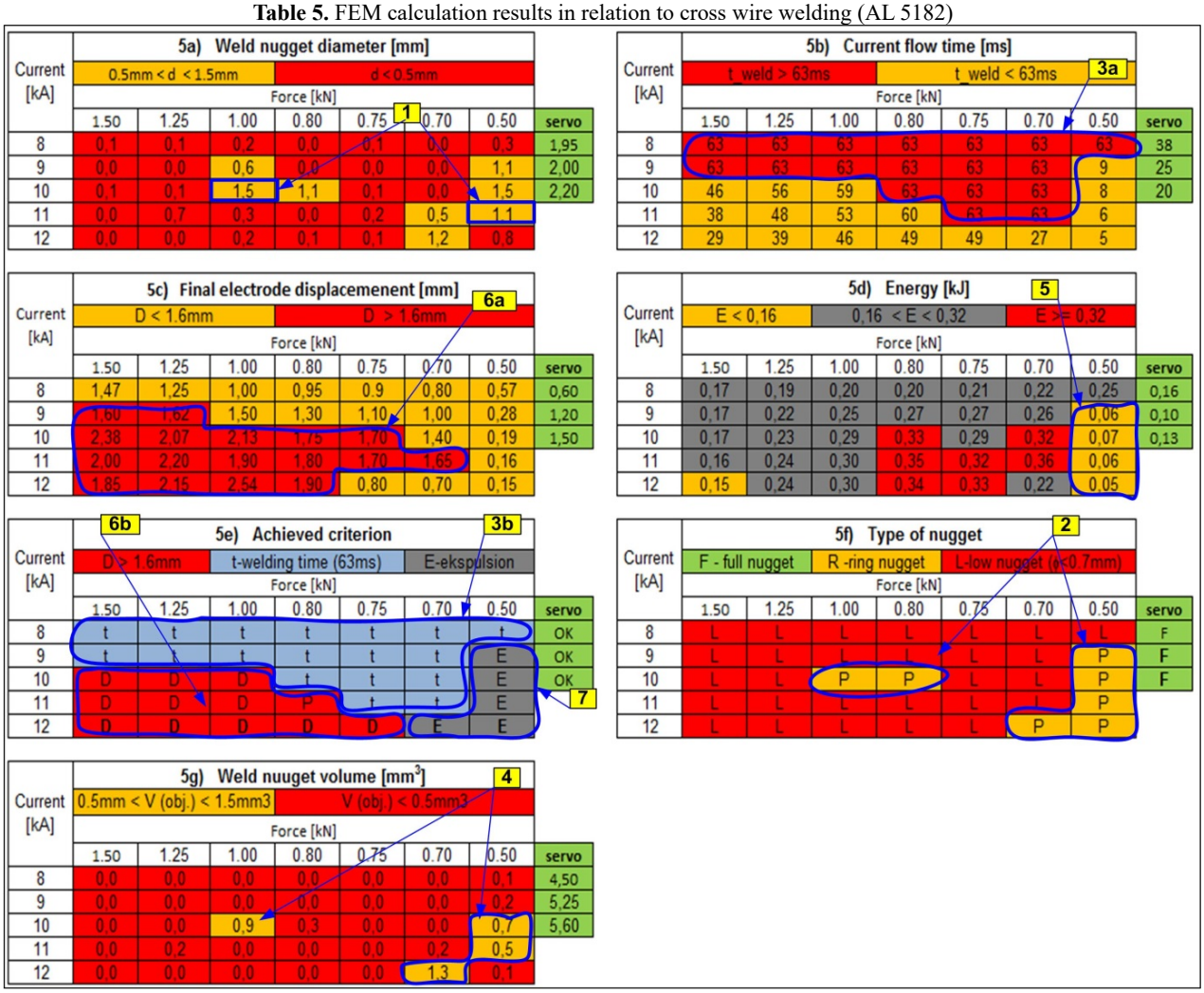

5a) Weld nugget diameter [mm]

Current [kA]	0.5mm < d < 1.5mm			d < 0.5mm				
	Force [kN]							
	1.50	1.25	1.00	0.80	0.75	0.70	0.50	servo
8	0,1	0,1	0,2	0,0	0,1	0,0	0,3	1,95
9	0,0	0,0	0,6	0,0	0,0	0,0	1,1	2,00
10	0,1	0,1	1,5	1,1	0,1	0,0	1,5	2,20
11	0,0	0,7	0,3	0,0	0,2	0,5	1,1	
12	0,0	0,0	0,2	0,1	0,1	1,2	0,8	

5b) Current flow time [ms]

Current [kA]	t_weld > 63ms			t_weld < 63ms				
	Force [kN]							
	1.50	1.25	1.00	0.80	0.75	0.70	0.50	servo
8	63	63	63	63	63	63	63	38
9	63	63	63	63	63	63	9	25
10	46	56	59	63	63	63	8	20
11	38	48	53	60	63	63	6	
12	29	39	46	49	49	27	5	

5c) Final electrode displacemenent [mm]

Current [kA]	D < 1.6mm					D > 1.6mm		
	Force [kN]							
	1.50	1.25	1.00	0.80	0.75	0.70	0.50	servo
8	1,47	1,25	1,00	0,95	0,9	0,80	0,57	0,60
9	1,60	1,62	1,50	1,30	1,10	1,00	0,28	1,20
10	2,38	2,07	2,13	1,75	1,70	1,40	0,19	1,50
11	2,00	2,20	1,90	1,80	1,70	1,65	0,16	
12	1,85	2,15	2,54	1,90	0,80	0,70	0,15	

5d) Energy [kJ]

Current [kA]	E < 0,16			0,16 < E < 0,32			E >= 0,32	
	Force [kN]							
	1.50	1.25	1.00	0.80	0.75	0.70	0.50	servo
8	0,17	0,19	0,20	0,20	0,21	0,22	0,25	0,16
9	0,17	0,22	0,25	0,27	0,27	0,26	0,06	0,10
10	0,17	0,23	0,29	0,33	0,29	0,32	0,07	0,13
11	0,16	0,24	0,30	0,35	0,32	0,36	0,06	
12	0,15	0,24	0,30	0,34	0,33	0,22	0,05	

5e) Achieved criterion

Current [kA]	D > 1.6mm			t-welding time (63ms)			E-ekspulsion	
	Force [kN]							
	1.50	1.25	1.00	0.80	0.75	0.70	0.50	servo
8	t	t	t	t	t	t	t	OK
9	t	t	t	t	t	t	E	OK
10	D	D	D	t	t	t	E	OK
11	D	D	D	P	t	t	E	
12	D	D	D	D	D	E	E	

5f) Type of nugget

Current [kA]	F - full nugget			R -ring nugget			L-low nugget (d<0.7mm)	
	Force [kN]							
	1.50	1.25	1.00	0.80	0.75	0.70	0.50	servo
8	L	L	L	L	L	L	L	F
9	L	L	L	L	L	L	P	F
10	L	L	P	P	L	L	P	F
11	L	L	L	L	L	L	P	
12	L	L	L	L	L	P	P	

5g) Weld nuuget volume [mm^3]

Current [kA]	0.5mm < V (obj.) < 1.5mm3			V (obj.) < 0.5mm3				
	Force [kN]							
	1.50	1.25	1.00	0.80	0.75	0.70	0.50	servo
8	0,0	0,0	0,0	0,0	0,0	0,0	0,1	4,50
9	0,0	0,0	0,0	0,0	0,0	0,0	0,2	5,25
10	0,0	0,0	0,9	0,3	0,0	0,0	0,7	5,60
11	0,0	0,2	0,0	0,0	0,0	0,2	0,5	
12	0,0	0,0	0,0	0,0	0,0	1,3	0,1	

– greatest volumes of molten (welded) metal were observed in relation to the highest values of welding current and the lowest values of electrode force (**Table 5g)**—parameter field 4). In relation to such welding parameters, the value of welding energy was relatively low (**Table 5d)**—parameter field 5). The welding time was very short and amounted to several milliseconds. A slight exceeding of the welding time creates the risk of expulsion (**Figure 5e)**—parameter field 7). The welding time was identified as a result of the exceeding of the criterion of the maximum temperature in the contact between the electrode and the material subjected to welding,

– above-standard penetration of wires, i.e., above the permissible value, was obtained in relation to lower values of welding current and higher values of electrode force (**Table 5c)**—parameter field 6a (final penetration) and **Table 5e)**—parameter field 6b (penetration amounting to $\Delta l = 1.6$ mm, obtained during the flow of current),

– risk of expulsion was observed in relation to the lowest value of electrode force and higher values of welding current (**Table 5e)**—parameter field 7).

However, the most important issue was the failure to satisfy the primary criterion, i.e., the nominal weld nugget diameter, set at 1.6 mm and the obtainment of the full weld nugget.

In addition, **Table 5** presents the results of the numerical calculations obtained in relation to the electromechanical electrode force system (green colour). All of the assumed criteria-related conditions were satisfied.

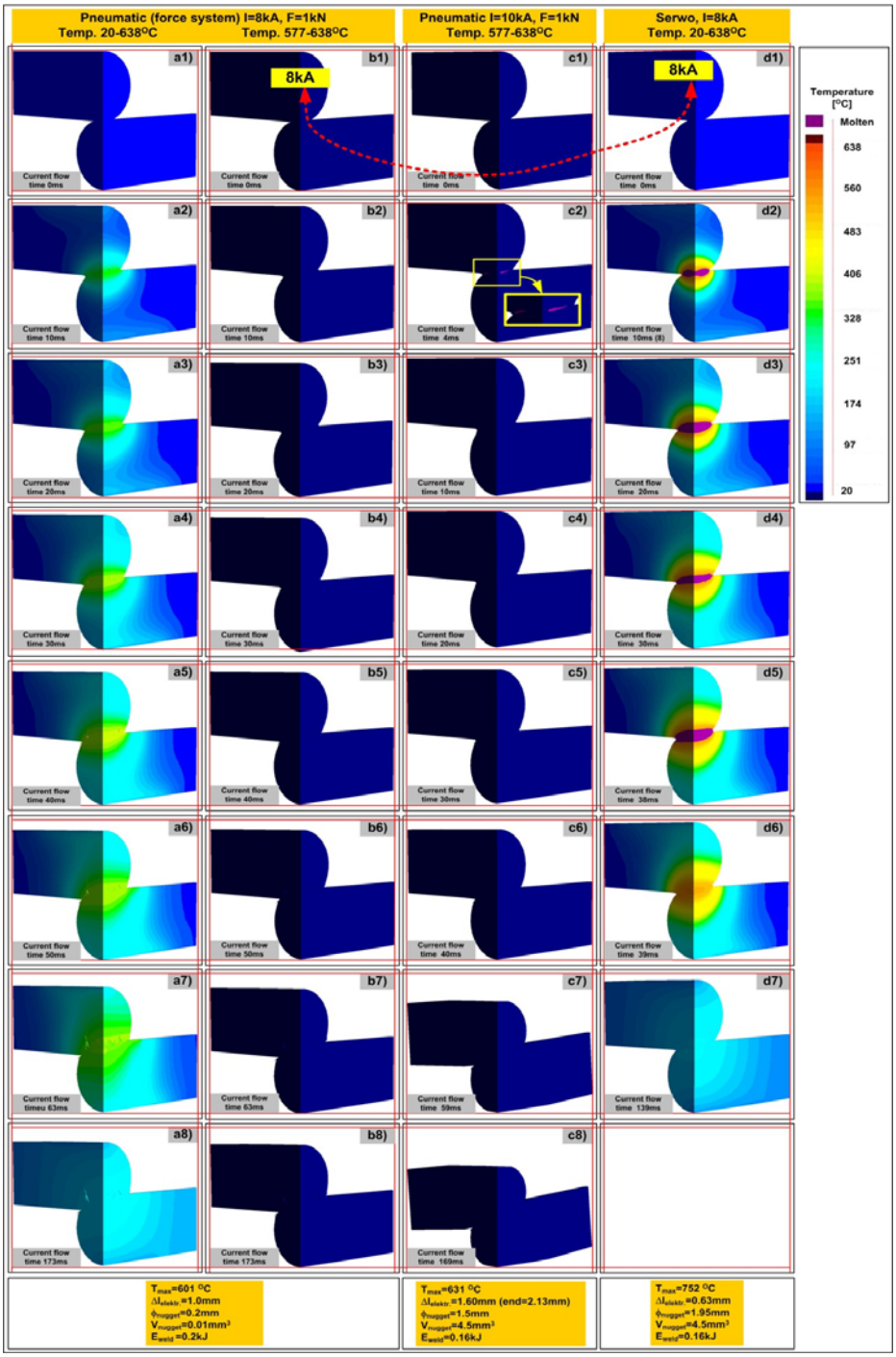

Figure 4. Temperature distribution in the welding area in relation to **a)/b)/c)** pneumatic force system (I = 8 kA and 10 kA, F = 1.0 kN) and **d)** electromechanical force system (I = 8.0 kA, servo force)

5.2 Comparison of PFS and EFS system

The comparison of the FEM calculation results and temperature distribution related to both, i.e., pneumatic and electromechanical, electrode force systems are presented in **Figure 4**. The presented test results are related to two selected welding current values, i.e., 8 kA and 10 kA.

In relation to the pneumatic force system and a welding current of 8 kA the distribution of temperature is presented within the entire range of temperature subjected to analysis, i.e., from ambient temperature to the melting point (liquidus) (**Figure 4a)**). In the above-named temperature range the melting of the metal was not observed and the weld nugget diameter calculated by the SOPRPAS software programme amounted to a mere of 0.2 mm. **Figure 4b)** presents the distribution of temperature within the range of solidus (577 °C) to liquidus (638 °C) tem-

perature. In the above-presented case, the melting of the material did not take place, which could imply that the joint was formed in the solid state in the entire contact (welding) area.

In relation to the higher current value, i.e., 10 kA, and the pneumatic force system, as a result of the welding area plasticisation and the effect of constant electrode force, molten metal was pushed outside. As a result, the contact area between welded materials (wires) grew excessively large, which, consequently, led to a significant decrease in current density and the immediate cooling of the weld material. The melting of the material was visible for a mere one millisecond (**Figure 4c2)**).

The temperature distribution results in relation to the electromechanical force system and a welding current value of 8 kA are presented in **Figure 4d)**. The entirely different manner of electrode force control led to the clearly visible melting of the material being welded and the formation of a full weld nugget (**Figure 4d)**). In the above case, the presentation of temperature distribution within the entire range of temperature subjected to analysis, i.e., from ambient temperature to the melting point (liquidus) (**Figure 4d)**) was very clear. In the analysed case of the welding of aluminium wires (Al 5182), the disconnection of power supply (current) resulted in the immediate (within 1 ms) reduction of temperature below the melting point (**Figure** 错误! 未找到引用源。**d5)–4d6)**). It should be mentioned that in relation to a welding current value of 8 kA and the pneumatic force system, the joint was obtained in the solid state in the entire welding area.

6. Process optimisation

The welding process optimisation was performed by comparing the courses of characteristic parameters (electrode displacement, momentary power, weld nugget diameter and electrode force) in relation to two electrode force systems (pneumatic and electromechanical) (**Figure 5**). The comparison was performed involving the same value of welding current, i.e., 8 kA. When the pneumatic system was used, the above-named value of welding current did not enable the obtainment of a proper weld. The melting of the material subjected to welding was little (or nearly not) visible (**Figure 4b)**). In turn, the use of the electromechanical system enabled the obtainment of a weld nugget having the previously assumed diameter, i.e., exceeding 1.6 mm (**Figure 4c)**).

Curves numbered 1 and 2 in **Figure 5** are concerned with the pneumatic system, whereas curves number 3 and 4 are related to the electromechanical system, where curves 2 and 4 present the waveforms of welding current (in relation to the pneumatic and electromechanical system respectively).

The course of the process performed using the pneumatic system can be described as follows. The pre-set constant electrode force (**Figure 5a)**, curve 1) as well as the specific value of welding current and the time of its flow (**Figure 5a)**, curve 2) generate specific welding power (**Figure 5b)**, curve 1) and the related displacement of electrodes (**Figure 5d)**, curve 1). The above-named factors lead to the obtainment of a weld nugget having a specific shape and dimensions (**Table 2**, **Figure 5c)**, curve 1), e.g., diameter of a mere 0.2 mm.

A welding current of 8 kA is overly low and is only responsible for the plasticisation of the material and the formation of the excessive contact area between elements subjected to welding. Current density is overly low and the melting of the material to be welded is not possible. The material in the contact area is only heated and plasticised. The maximum welding time amounting to 63 ms is exceeded and the related criterion is not satisfied.

The initial stage of the cross-wire welding optimisation involved an appropriate change in the course of electrode displacement (wire penetration depth) (**Figure 5d)**) (curve No. 3) resulting from the use of the electromechanical force system and from the application of an appropriate electrode displacement control algorithm. The essence of the change in the course of electrode displacement involved the direct control of this parameter, particularly during the flow of welding current. In general, it is necessary to slow down the process of electrode displacement in order to obtain more favourable power density distribution and to generate higher welding power (**Figure 5b)**, curve 3) in comparison with those obtained during welding performed using the pneumatic system. Slower electrode displacement accompanied by constant

welding current increases resistance in the contact area, leading to an increase in welding power. As a result, the sequence of events is the following: (1) contact area between elements being welded is smaller, (2) resistance in the contact is higher and (3) temperature distribution in the welding area is more favourable. All of the above-named factors enable the obtainment of a weld nugget having a diameter exceeding 1.6 mm (**Figure 5c)**, curve 3).

The final effect of the above-presented manner of control is the appropriate course of electrode force (**Figure 5a)**, curve 3). Electrode force affects the value of resistance, particularly in the contact areas (especially in the welded wire-welded wire configuration), which, in turn, is responsible for the appropriate space distribution of power and welding energy. Consequently, the foregoing translates into the appropriate distribution of temperature in the welding area, leading to the melting of a material subjected to welding and enabling the formation of a weld of appropriately greater diameter.

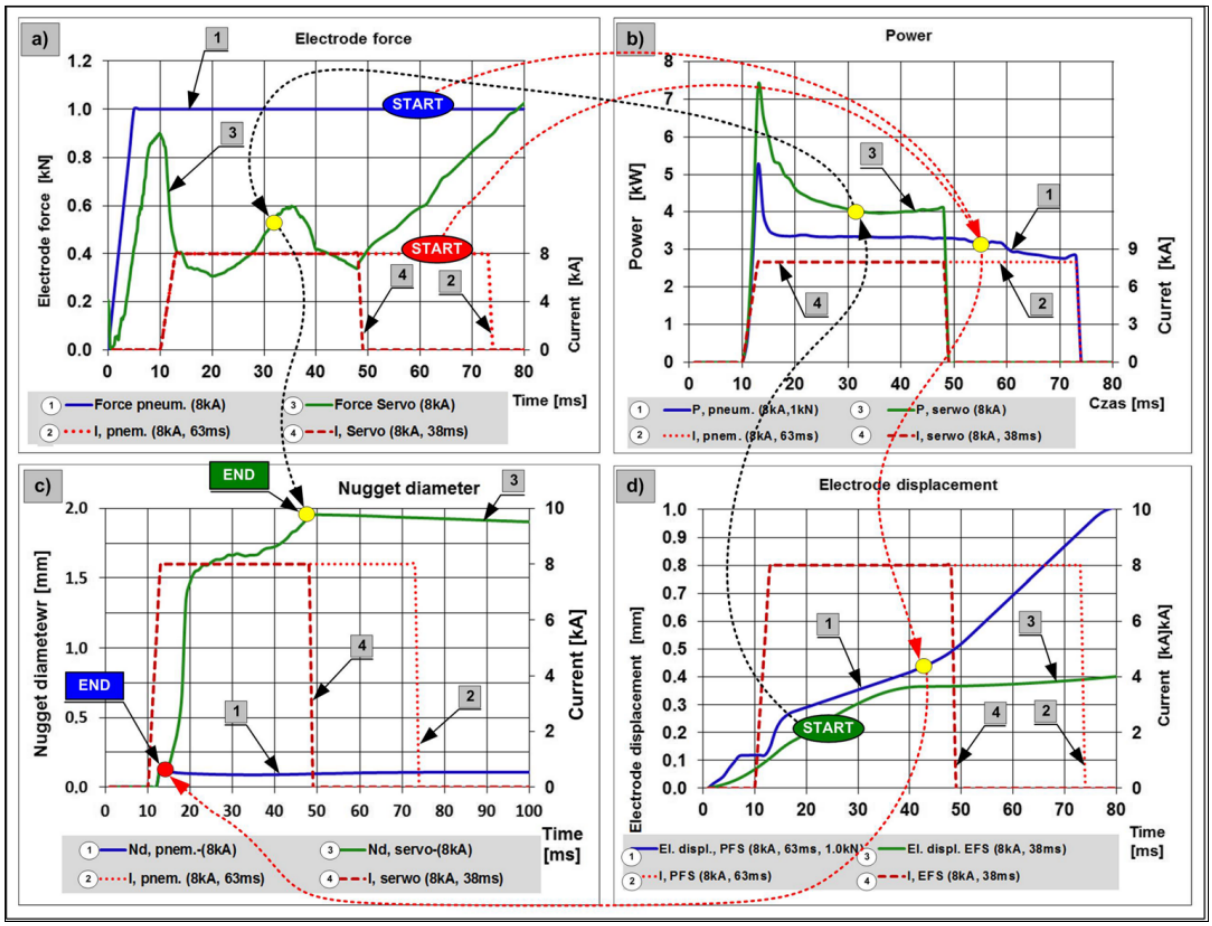

Figure 5. FEM calculation results: **a)** electrode force; **b)** momentary power; **c)** electrode displacement (wire penetration depth); **d)** weld nugget diameter; curves 1 and 2 PFS (I = 8.0 kA, F = 1.0 kN); curves 3 and 4 EFS (I = 8.0 kA, servo force)**.**

When summarizing this part of analysis related to the value of welding current amounting to 8.0 kA (and recognised as overly low to obtain a proper joint using the pneumatic force system)), it is necessary to state that the use of the electromechanical system and appropriate electrode force and/or displacement control significantly improve the quality of a welding process and enable the obtainment of a full weld nugget having the previously assumed diameter (>1.6 mm) (obviously after satisfying the remaining requirements (quality criteria).

The results presented in **Figure 5** were obtained on the basis of calculations performed using the SORPAS 3D model.

7. Experimental verification

Experimental tests were performed using test rigs equipped with DC inverter welding machines (DC 1 kHz) – **Figure 6**. The electric parameters of the welding process were recorded using the Log-

Weld 4 device (**Figure 7**).

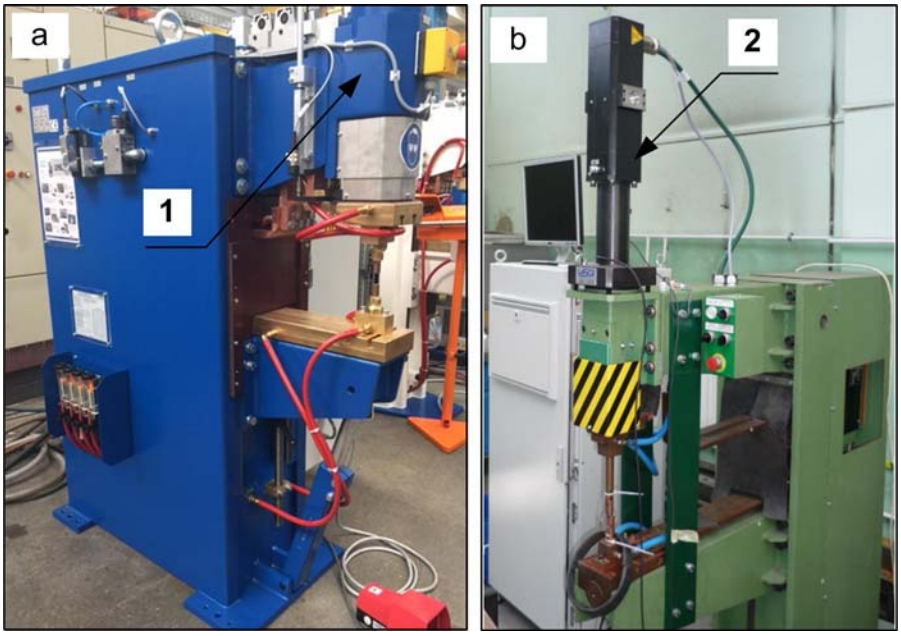

Figure 6. Test station for technological welding tests performed using: **a)** pneumatic and **b)** electromechanical electrode force; (1) pneumatic actuator, (2) servo-motor**.**

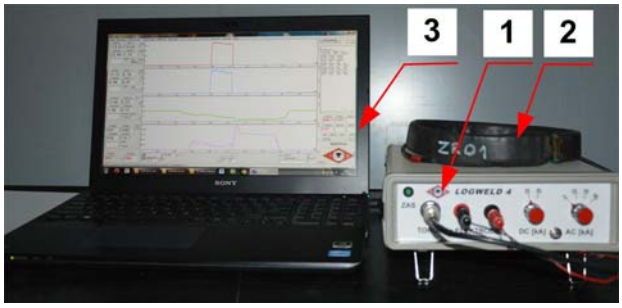

Figure 7. LogWeld measurement device 4 for measurements of characteristic parameters of the resistance welding process (welding current and voltage, electrode force and displacement); (1) measurement interface, (2) toroid, (3) PC

The numerical calculation results were verified experimentally. The experimental tests were performed in relation to the nine variants presented in **Table 4** and concerning the pneumatic force system. Destructive (peeling) tests confirmed the formation of a ring weld in each of the variants (P1 through P9). None of the variants related to the pneumatic force system satisfied the previously assumed criteria. Variant P5 was considered as *the closest* to the most favourable welding conditions. Further technological welding tests (**Table 6**: variant PE1 and PE2) were performed in relation to parameters similar to variant P5 (**Table 4**). The results concerning the pre-set parameters and the parameters characteristic of technological welding tests in relation to the pneumatic force system (variant PE1 and PE2) are presented in **Table 6**, whereas the results in the form of a joint structure are presented in **Figure 8a)**. The electric parameters of the welding process, i.e. welding current and voltage were recorded using the LogWeld 4 measurement device.

The technological parameters related to variants PE1 and PE2 were the following: (1) force F= 1.0 kN, (2) welding current I = 9.5–10 kA and (3) welding time t = 40–70 ms. In relation to the above-presented welding technology parameters, the FEM calculation results indicated the obtainment of a weld nugget having the greatest diameter (1.5 mm), yet still being ring-shaped. Metallographic tests confirmed the results obtained in the numerical calculations, i.e. the formation of a ring weld.

Table 6. Pre-set parameters and parameters characteristic of the pneumatic electrode force system

No.	Variant no.	Present parameters					Recorded parameters				
		Electrode force	Up-slope		Main welding time		Total current (I_{rms})	Energy	Wire penetration	Weld diameter	Number of tests
			Current	Time	Current	Time					
		kN	kA	ms	kA	ms	kA	kJ	mm	mm	pcs
		A	B1	B2	C1	C2	D	E	F	G	H
1	PE1	1.0	10.0	3	10.0	40-60	10.0	0.23	1.50	1.5	20
2	PE2	1.0	9.5	3	9.5	50-70	9.5	0.21	1.38	1.3	20

Afterwards, the welding process was subjected to optimisation by using lower welding current values restricted within the range of 8.0 to 8.5 kA and an appropriate force profile involving the use of the electromechanical system (**Table 7**: variant EE1 and EE2). The results concerning the pre-set parameters and the parameters characteristic of technological welding tests in relation to the electromechanical force system are presented in **Table 7**, whereas the results in the form of a joint structure are presented in **Figure 8b**. The electric parameters of the process, i.e., welding current and voltage were recorded using the LogWeld 4 measurement device

Table 7. Pre-set parameters and parameters characteristic of the electromechanical electrode force system

No.	Variant no.	Present parameters								Recorded parameters							
		Force			Up-slope		Main welding time		Total current	Electrode displacement and time				Energy	Bar penetration	Weld diameter	Number of tests
		Initial	Min.	Max.	Cur.	Time	Cur.	Time		T_1/ Δl_1	T_2/ Δl_2	T_3/ Δl_3	T_4/ Δl_4				
		kN			kA	ms	kA	ms	kA	ms/mm				kJ	mm	mm	pcs
		A1	A2	A3	B1	B2	C1	C2	D	E0	E1	E2	E3	F	G	H	I
1	EE1	1.0	0.4	1.0	8.0	3	8.0	45	8.0	10 0.08	30 0.25	10 0.05	30 0.25	0.16	0.70	1.87	20
2	EE2	1.0	0.4	1.0	8.5	3	8.5	40	8.5	10 0.08	25 0.25	7 0.05	30 0.25	0.20	0.75	1.92	20

I_{rms} root-mean-square current, EE electromechanical experiment

Figure 8b presents the melting of the welded materials in the entire weld area. Importantly, the melting of the material also took place in the central part of the joint.

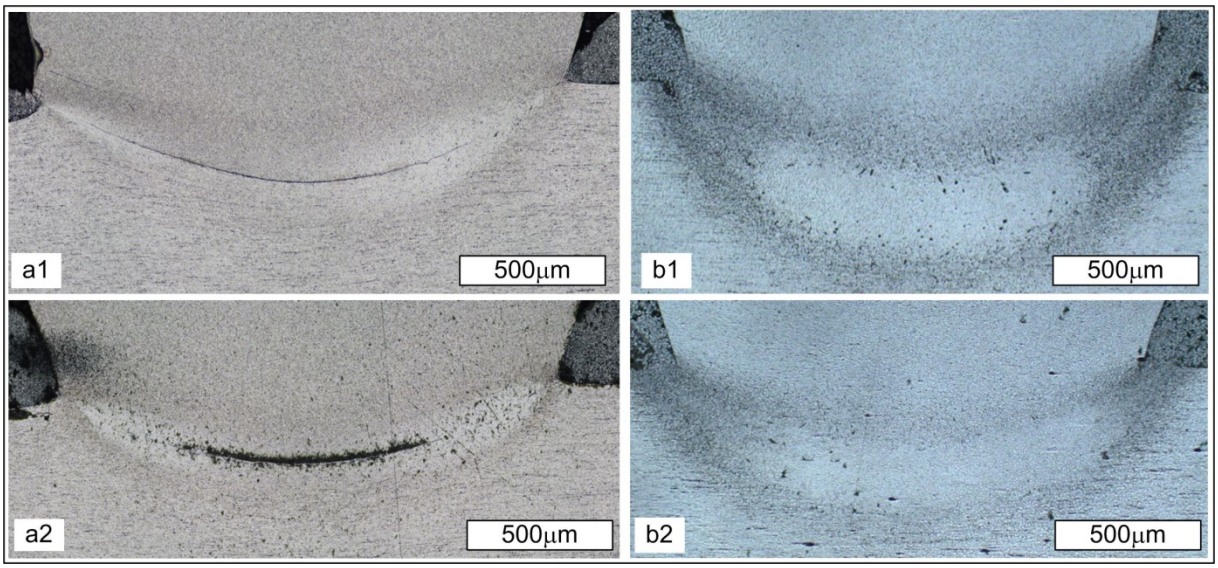

Figure 8. Metallographic test results: **a** PFS **a1** variant PE1, **a2** variant PE2, **b** EFS **b1** variant EE1, **b2** variant EE2

8. Conclusions

The adjustment of the most favourable parameters of the cross-wire projection welding technol-

ogy involving the use of the pneumatic electrode force system, particularly in relation to soft materials, e.g., aluminium alloys, proves very difficult (nearly impossible). In the case of the aforesaid force system, the electrode force is excessively high in relation to short welding time and high welding current. The above-named conditions are in conflict and constitute significant limitations to the adjustment of welding parameters. The primary limitation is the dynamics of the electrode force system, i.e., the lack of the possibility of fast electrode force control within a short time of current flow.

A characteristic of the pneumatic force system is the fact that (electrode) force is a pre-set parameter, whereas the resultant parameter is the displacement of electrodes, not controlled on any manner.

The improvement of the welding process course (extension of the parameter window) requires the use of the electromechanical electrode force system. During operation involving the displacement of electrodes it is possible to adjust more favourable electrode displacement trajectory enabling the obtainment of more favourable current density distribution, more favourable space distribution of welding power, generation of higher energy in the central zone of a joint, generation of significantly higher temperature in the aforesaid area and, finally, the obtainment of a larger weld.

The use of the electromechanical force system makes it possible to control the displacement of electrodes during the flow of current as well as to obtain the assumed final displacement of electrodes resulting in the obtainment of specific (smaller) projection height reduction.

Acknowledgments

This work was supported by the Polish National Centre for Research and Development (NCBR) under project no. TANGO1/267374/NCBR/2015.

Conflict of interest

The authors declared that they have no conflict of interest.

References

1. Zhang H, Senkara J. Resitance welding fundamentals and applications. Taylor&Francis Group; 2011.
2. Zhang X, Chen G, Zhang Y, *et al*. Improvement of resistance spot weldability for dual-phase (DP600) steels using servo gun. Journal of Materials Processing Technology 2009; 209: 2671–2675.
3. Tang H, Hou W, Hu S. Forging force in resistance spot welding. Proceedings of the Institution of Mechanical Engineers, Part B: Journal of Engineering Manufacture 2002; 216(7): 957–968.
4. Gould J. Joining Aluminum Sheet in the Automotive Industry—A 30-year history. Welding Journal (Welding Research) 2012; 91: 23–34.
5. Zhang X, Chen G, Zhang Y. On-line evaluation of electrode wear by servo gun. International Journal of Advanced Manufacturing Technology 2008; 36.
6. Slavick SA. Using servo guns for automated resistance welding. Welding Journal 1999; 78(7): 29–32.
7. Mikno Z. Projection welding with pneumatic and servomechanical electrode operating force systems. Welding Journal (Welding Research) 2016; 95: 286-299.
8. Mikno Z, StepieńM, Grzesik B. Optimization of resistance welding by using an electric servo actuator. Welding in the World 2017; 61: 453–462. DOI:10.1007/s40194-017-0437-x.
9. Mikno Z, Bartnik Z, Ambroziak A, *et al.* (inventors) Method for Projection Resistance Welding of Steel Plates with Embossed Projections. Polish patent. 401723. 2012.
10. Mikno Z, Grzesik B, Stępień M (inventors). A manner of resistance projection welding in configuration of the cross, mainly for aluminium wires. Polish Patent. 412615. 2015.
11. The database of the material and electrode parameters: model 3D Version 4.0x64 of the Swantec Inc. SORPAS Software. http://swantec.com/
12. Papkala H. Resistance welding of metals. Publishing House KaBe Krosno; 2003.
13. AWS Welding Handbook 9th ed, vol. 3, welding processes, part 2 chapter 2, projection welding.
14. Projection Welding, Gould JE. Welding, Brazing, and Soldering (USA). ASM International, ASM Handbook. 1993. 230–237.
15. Statistica 12. www.statsoft.pl.